NAVAL POSTGRADUATE SCHOOL
Monterey, California

THESIS

LIQUID CRYSTAL MAPPING OF
JET CROSSFLOW INTERACTIONS

by

Michael David Johnson

December 1981

Thesis Advisor: R. H. Nunn

REPORT DOCUMENTATION PAGE

READ INSTRUCTIONS BEFORE COMPLETING FORM

1. REPORT NUMBER
2. GOVT ACCESSION NO.
3. RECIPIENT'S CATALOG NUMBER

4. TITLE (and Subtitle)

Liquid Crystal Mapping of Jet-Crossflow Interactions

5. TYPE OF REPORT & PERIOD COVERED

Master's Thesis
December 1981

6. PERFORMING ORG. REPORT NUMBER

7. AUTHOR(s)

Michael David Johnson

8. CONTRACT OR GRANT NUMBER(s)

9. PERFORMING ORGANIZATION NAME AND ADDRESS

Naval Postgraduate School
Monterey, California 93940

10. PROGRAM ELEMENT, PROJECT, TASK AREA & WORK UNIT NUMBERS

11. CONTROLLING OFFICE NAME AND ADDRESS

Naval Postgraduate School
Monterey, California 93940

12. REPORT DATE

December 1981

13. NUMBER OF PAGES

61

14. MONITORING AGENCY NAME & ADDRESS(if different from Controlling Office)

15. SECURITY CLASS. (of this report)

Unclassified

15a. DECLASSIFICATION/DOWNGRADING SCHEDULE

16. DISTRIBUTION STATEMENT (of this Report)

Approved for public release, distribution unlimited.

17. DISTRIBUTION STATEMENT (of the abstract entered in Block 20, if different from Report)

18. SUPPLEMENTARY NOTES

19. KEY WORDS (Continue on reverse side if necessary and identify by block number)

Liquid crystals, Thermography, Lateral thrust units, Bow thruster, Jet-crossflow interaction, Jets in crossflow, Isotherms, Flat plate.

20. ABSTRACT (Continue on reverse side if necessary and identify by block number)

The use of liquid crystal thermography is discussed as a technique for visualizing the disturbance field created on a surface from which a jet is injected into a crossing flow. The study is part of an ongoing investigation of the performance of jet steering systems such as ship bow thrusters. An experimental apparatus was designed and built to provide a heated surface coated with liquid crystals. For a range of

20. ABSTRACT (Continued)

jet-to-crossflow velocity ratios, the temperature field on the flat plate was visually represented. The technique allowed continual visual observation of the cooling effects of the jet as jet velocity increased. It also showed the cooling pattern similarities that exist at the same velocity ratios for different crossflow velocities. Strong visual similarities were shown to exist between the temperature distribution on the flat plate as depicted by the liquid crystals and the theoretical surface velocity field around a jet modelled as a symmetrical foil near the point of injection and a vortex sheet in the plumes.

Approved for public release, distribution unlimited.

Liquid Crystal Mapping of Jet Crossflow Interactions

by

Michael David Johnson
Lieutenant, United States Navy
B.S., United States Naval Academy, 1975

Submitted in partial fulfillment of the
requirements for the degree of

MASTER OF SCIENCE IN MECHANICAL ENGINEERING

from the

NAVAL POSTGRADUATE SCHOOL
December 1981

ABSTRACT

The use of liquid crystal thermography is discussed as a technique for visualizing the disturbance field created on a surface from which a jet is injected into a crossing flow. The study is part of an ongoing investigation of the performance of jet steering systems such as ship bow thrusters. An experimental apparatus was designed and built to provide a heated surface coated with liquid crystals. For a range of jet-to-crossflow velocity ratios, the temperature field on the flat plate was visually represented. The technique allowed continual visual observation of the cooling effects of the jet as jet velocity increased. It also showed the cooling pattern similarities that exist at the same velocity ratios for different crossflow velocities. Strong visual similarities were shown to exist between the temperature distribution on the flat plate as depicted by the liquid crystals and the theoretical surface velocity field around a jet modelled as a symmetrical foil near the point of injection and a vortex sheet in the plumes.

TABLE OF CONTENTS

LIST OF TABLES

LIST OF FIGURES

LIST OF SYMBOLS

A - Area

h - Heat transfer coefficient

m - Jet-to-crossflow ratio

Q - Heat transfer rate

Re - Reynolds number

ΔT - Temperature difference between plate surface and free steam

U_∞ - Crossflow velocity

ACKNOWLEDGEMENTS

The author wishes to express his appreciation to Professor Robert H. Nunn for his advice and guidance during the development of this study. The helpful advice on liquid crystal thermography provided by Professor Matthew D. Kelleher was also greatly appreciated.

Many thanks to my wife, Glynda, for her patience and understanding during the long hours needed to complete this study.

I. INTRODUCTION

Having the power to turn a ship in order to direct the ship's head to any given point has long been the desire of the ship driver [1]. Traditionally, ships have been steered by the use of rudders and rudder-like devices mounted on the stern and leaving the bow relatively uncontrolled. This system has always led to poor maneuverability at low speeds due to low water velocities at the rudder. Another major problem was the lack of maneuverability in confined waterways and in docking. As the size of the ship increased, so did the problem.

The development of active maneuvering devices, or thrusters, has enabled vessels to achieve a higher degree of maneuverability and independence. These devices are installed in the bow or stern of the ship in order to produce a controllable side thrust on the ship. The most common maneuvering and control capability required of the thruster is when the ship is dead in the water or at extremely low speed and desires to change heading or maintain its head. The action of the thruster is to produce a jet of water which is injected into the surrounding water. This thrusting action swings the ship bodily, or may be used to hold the ship against an external influence such as wind and current.

Considering the large number of ships already fitted with thrust units, it seems rather surprising that little pre-installation design has been undertaken. Thruster sizing is routinely accomplished by comparison with other units of successful performance, reliability, reasonable cost, and personal preference [2,3]. The performance of some bow thrusters could probably have been improved if more performance parameters had been available and design criteria defined during their design. The limited testing that has been undertaken identifies contradictions that exist as to the changes in the effectiveness of the thrust unit with minor changes in speed.

The injection of a high velocity jet into a crossflow, which best describes the action of the thrust unit, produces a complicated flow field. A review of the literature has revealed that the primary interest in this kind of flow phenomenon has been in the area of aircraft jet thrust systems such as those deployed on Vertical/Short Take-off and Landing Aircraft (V/STOL). Traditionally, investigators have attempted to study this complicated flow field by concentrating on a simplified model in which a round jet is exhausted perpendicularly through a flat plate into the crossflow. Experiments have concentrated on several aspects of this jet-in-a-crossflow problem; particularly, defining the jet trajectory [4-11] and identifying the pressure distribution on the flat plate [3, 12-18].

One motivation for studying a jet in a crossflow is to develop an understanding of the pressure distribution on the flat plate through which it exhausts. In their investigations, English [3] and Chislett and Bjorheden [19] noted that the interaction of the jet with the crossflow gave rise to suction forces to the sides and behind the jet. The ability to predict the magnitude of this suction force and its center of action would permit designers to more accurately determine powering and control requirements for thrusters. Theoretically, the characteristics of the thruster could be predicted by incorporating a mathematical model for calculating the pressure distribution on the flat plate. Attempts to formulate such models have been described in Refs. 20-22.

The primary purpose of this study is to provide a visual representation of the surface flow field utilizing the temperature distribution on the flat plate created by the interaction of the jet and crossflow. Ultimately, it is anticipated that a relationship between temperature distribution and pressure distribution will be developed in order to facilitate the prediction of the magnitude and center of action of the suction forces on the flat plate.

II. BACKGROUND

A. BOW THRUSTERS

It has been the experience of the author that bow thrusters are a very useful maneuvering tool, though somewhat unpredictable. Use of the bow thruster on tank landing ships (LST) is an operational necessity because of the mission of the ship. Routine operations include actual beaching of the ship and marrying end-on to floating pontoon bridges. Both are low speed operations requiring high maneuverability. The LST driver quickly learns two "rules of thumb" when operating the bow thruster. One, the bow thruster is ineffective at ship speeds above five knots; and two, if at first one does not achieve the desired thrust effect, change the thruster power until one does. It is conjectured that the reason for the second "rule" is to offset the external effects of wind and current and no further explanations are necessary or desired by the operator.

Realistically, this is not the case. As has been mentioned, there is a confusing and complicated flow field produced by the jet-crossflow interaction. A short account of the physical processes taking place may be necessary for a better understanding of these interactions between jet and crossflow.

A circular jet of fluid discharged normally from a flat plate into a crossflowing stream will obviously be deflected into the direction of the crossflow. For a given crossflow velocity, the penetration and deflection is closely linked to the velocity of the jet. This has been confirmed by experiment [4-12] where the paths of jets have been determined utilizing the single parameter

$$\text{velocity ratio, } m = \frac{\text{jet velocity}}{\text{crossflow velocity}} .$$

English [3] has described the reasons for the turning of the jet. There exists a low pressure wake behind the jet, while the pressure ahead of the jet tends to, but does not reach the stagnation value of the crossflow. The difference in these pressures causes the jet to bend downstream into the crossflow direction. The development of the shear layer at the periphery of the jet continues as the jet advances into the mainstream. Since this is a layer of lower velocity than the jet core, it is easily deflected. This becomes the dominant factor in the bending process as the distance from the jet origin increases. The jet cross-section gradually changes shape from the circular form to a horseshoe or kidney shape.

Experiments with thrust units have been restricted to investigating the effect of forward speed on side thrust and body turning moment created by the thruster [3,19,23-25], and identifying a proper design procedure which permits

selection of a practical thrust unit [26-28]. The following background comments are representative of the quantity and scope of published information on the subject.

English [3] has made measurements of pressure forces on a flat plate with a jet exhausting normally from the plate into a crossflow in a circulating water channel. He subsequently evaluated thruster performance on a model hull by measuring side forces at various ship model speeds and pressure changes caused by the jet stream interaction on the hull.

Stuntz and Taylor [23] have studied the designs of tunnel ends in order to try to increase thrust for a minimun increase in hull resistance. They have demonstrated how the use of fences and bars placed across the tunnel entrance reduces resistance in some cases.

Chislett and Bjorheden [19] have made measurements of side thrust and body turning moment on a model hull. Their tests have shown that with increasing ahead spead, the turning moment on the ship due to the thruster is reduced and reaches its lowest value in the region of 2 to 5 knots, depending upon the length of the vessel. Special attention was given to explaining the effect of the ratio of model speed to thruster jet velocity.

Norrby [24] has measured side force and turning moment on a large ship model. He has mentioned a few tests which

indicate that the body moment from a thruster is increased at a drift angle, as in a turn, in comparison to the no drift angle case. Also, for a ship with both bow thruster and rudder, he has found the maneuverability considerably higher than for a ship with rudder only.

Beveridge [25] has conducted wind tunnel pressure tests and flow visualization experiments to determine the characteristics of the outflow of the thruster jet. He has examined, both experimentally and theoretically, the interaction between the ambient flow and bow thruster inflow and outflow. The performance of different sized bow thrusters was compared, and indicated that a smaller diameter duct produces less suction force than a larger diameter duct.

English [26] has introduced a static merit coefficient to predict thruster efficiency. An analytical study of duct inlet shapes has also been made.

Dewhurst [27] has suggested a method for establishing an initial choice of power for thruster installations. He has developed a method of selection that gives a good first approximation with a minimum of calculation.

Beveridge [28] has confirmed the major interaction effect created by the thruster outflow at large distances downstream. Additionally, he has developed a step-by-step design procedure for selection of a bow thruster. Some of the details presented include recommendations for duct immersion, duct diameter, duct length, propeller blade shape, and propeller pitch-diameter ratio.

In an attempt to gain a greater insight into the flow phenomenon created by discharging the jet into the crossflow, the literature search was expanded into the area of aircraft jet thruster systems -a closely related field. The problem involved in using jets to provide the necessary thrust for V/STOL aircraft take-off led Jordinson [4] to conduct experiments on the discharge of a jet from an orifice into a crossing airstream. These were the first relevant experiments on the problem. A second experimental study by Gordier [5] over the same general range of velocity ratios was the first to be carried out in a water tunnel.

The problem has been extended further, both experimentally and analytically, by a number of investigators. Keffer and Baines [6] presented experimental results from which it was determined that for various jet strengths, jet trajectories could be represented by a single function. Margason [7] utilized flow visualization techniques and pressure measurements to formulate a trajectory equation. Sucec and Bowley [11] formulated an analytical expression for the jet trajectory utilizing previous experimental information and the assumption that the distributed pressure force and entrained momentum flux could be approximated by an aerodynamic drag force.

The ability to predict the jet trajectory is of definite importance, but the primary objective of the present study is to provide insight into the changes in the otherwise uniform

flow created by the discharge of the jet. Experiments conducted by Vogler [12], Bradbury and Wood [13], McMahon and Mosler [15], Kamotani and Greber [16], Fearn and Weston [17], and others provide measured values of the pressure distribution on the surface surrounding the jet. These pressure distributions will be useful for comparisons with visual temperature distributions created on the flat plate by the jet-crossflow interaction in an attempt to develop a relationship between the two.

B. LIQUID CRYSTALS

Liquid crystals are substances that share some of the physical properties of both liquids and solids. They exhibit an intermediate phase between the pure solid phase and the pure liquid phase, appropriately termed a "liquid crystal phase" [29]. They resemble liquids in the mechanical sense and crystals in the optical sense. The molecular structure of the liquid crystal determines its classification: either smectic, nematic, or cholesteric.

Cholesteric liquid crystals are formed from polymers of cholesterol. The structure of the cholesteric liquid crystal is so delicately balanced that, when disturbed, it produces an optical transformation. When applied to a black subsurface, the cholesteric liquid crystal progressively exhibits the colors of the visible spectrum over discrete, reproducible and reversible temperature bands. This process is unique for

each liquid crystal since each has a particular range of sensitivity. Used as a temperature sensor, liquid crystals allow one to visually observe selected isotherms.

Early use of liquid crystals in wind tunnel experiments [30] led to the conclusion that pure liquid crystals deteriorate rapidly with age and are susceptible to contamination, ultraviolet light, and mechanical shear. This led to the development of encapsulated liquid crystals by the National Cash Register Company (NCR). The encapsulated liquid crystals are coated with gelatin in a polyvinyl alcohol binder. This coating results in small spheroids with diameters on the order of 20-50 microns which remain unaffected by contaminants, ultraviolet light, and shear stresses [31].

Previous work with liquid crystals has attempted to determine boundary layer translation, flow separation points, and heat transfer in cylinders, ducts, and other bodies [32-35]. The present investigation will utilize the liquid crystals applied to a flat plate through which a jet is discharged into a crossflow to visualize the temperature on the flat plate created by the jet-crossflow interaction.

III. DESCRIPTION OF APPARATUS

A. LIQUID CRYSTALS

Since each liquid crystal has its own sensitivity and is colorless above and below its operating range, by selecting the proper formulation of crystals a large number of isotherms can be viewed on a given surface at one time. Cholerestic liquid crystals are divided into three categories: S- or short range, with approximately a two degree temperature band of activity, R- or regular range, with a three to five degree temperature band; and W- or wide range, with greater than a five degree temperature band. An example would be the liquid crystal S-40 (40 being the temperature in degrees Celsius at which the onset of red appears). As the temperature is raised to 40.0°C, the colorless liquid crystals start to show red. The color begins to shift to green at 40.7°C, then to blue at 41.3°C, and finally to violet prior to becoming colorless again.

A mixture of four separate liquid crystal formulations was used in the present study. A temperature range of 83°F to 103°F was covered. A water-filled Rosemount constant temperature calibration bath, capable of establishing and maintaining temperatures to within 0.01°F accuracy, was employed in the liquid crystal calibration procedure. All liquid crystals were calibrated on a piece of the material to which

they would be applied for data collection. The general procedure outlined in Ref. 31 was followed. Table I lists the liquid crystals used and the calibration results.

TABLE I

LIQUID CRYSTAL CALIBRATION RESULTS

Liquid Crystal (NCR Designation)	Color Transition		
	Red (°F)	Green (°F)	Blue (°F)
S-30	83.6	84.5	86.2
S-32	89.9	90.7	92.0
S-34	93.7	94.5	95.4
R-37	98.8	100.7	102.2

B. FLAT PLATE

Figures 1 and 2 show the details of the flat plate construction. The flat plate is 1/2 inch thick plexiglas, 20 inches long, and 9-7/8 inches wide with a sharp leading edge. A brass nozzle, 3/4 inch outside diameter and 1/4 inch inside diameter, was mounted into the plate. The area around the nozzle was covered with an electrically resistive carbon impregnated paper (Temsheet) and the liquid crystals were applied directly to this Temsheet. The flat plate was held parallel to the oncoming flow in the center of the wind tunnel by two plexiglas side panels.

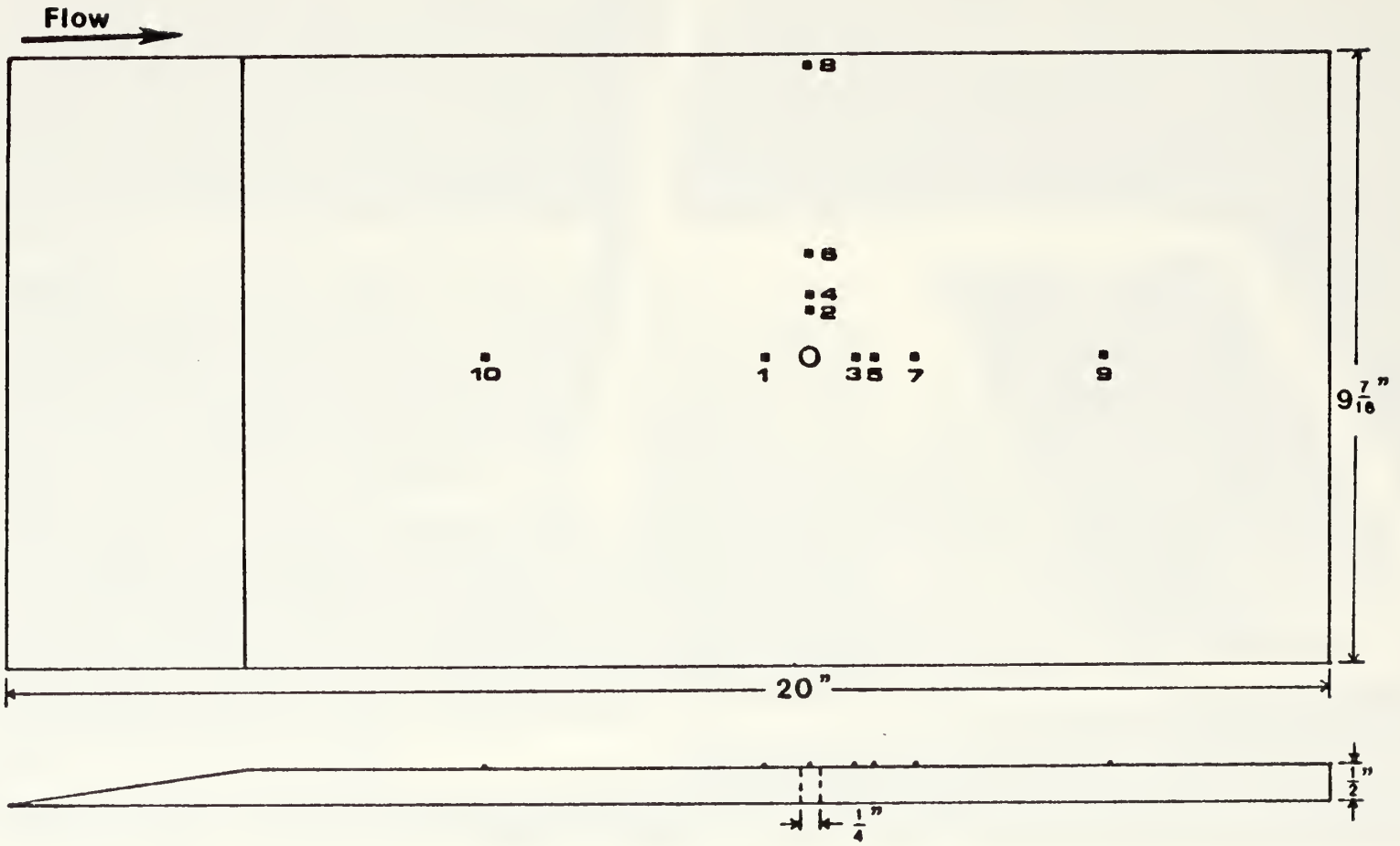

Figure 1. Details of Flat Plate and Thermocouple Locations.

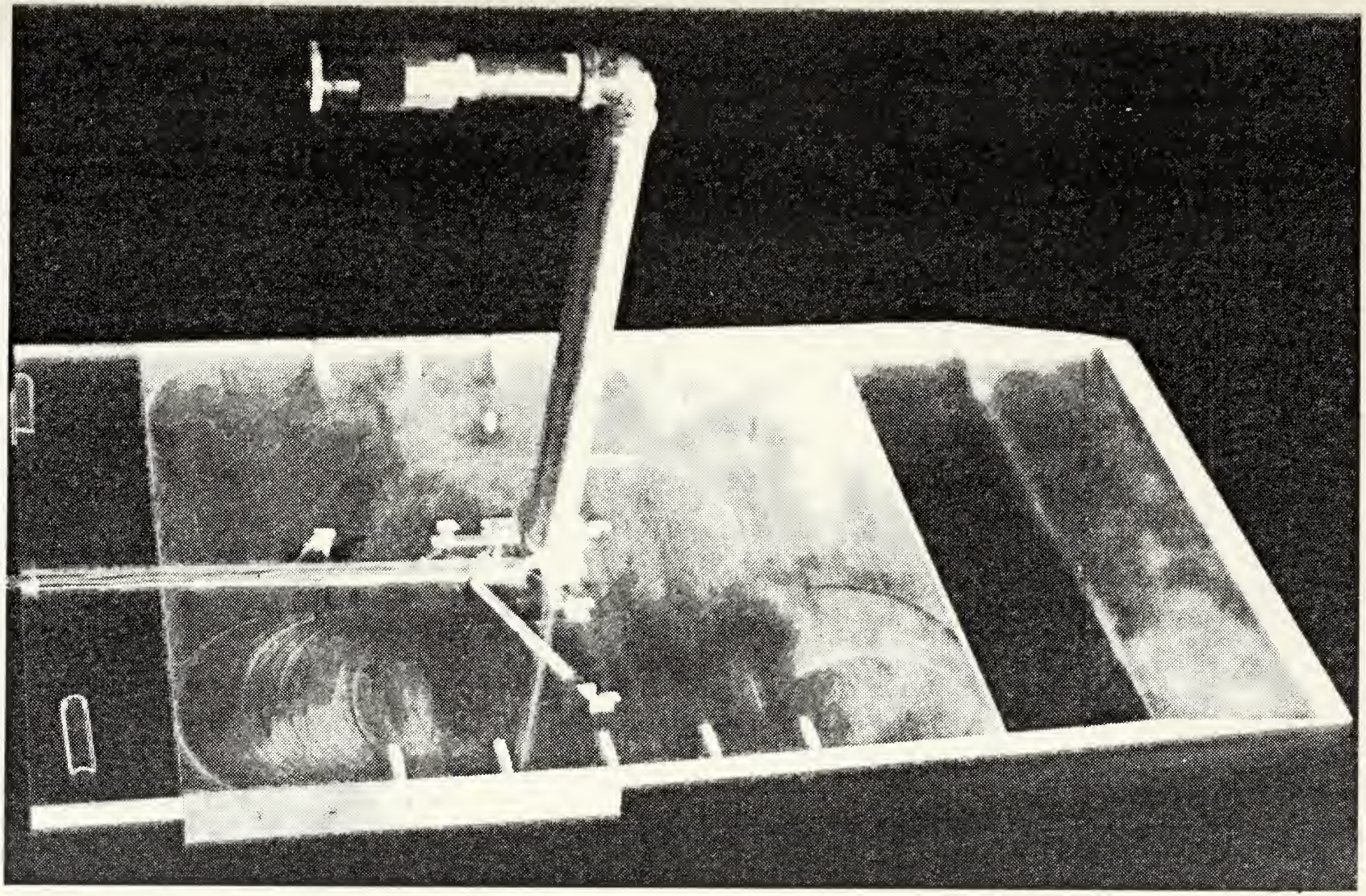

Figure 2. Upper View of Flat Plate with Nozzle.

C. LOW TURBULENCE SUBSONIC WIND TUNNEL

The low turbulence subsonic wind tunnel is of an open circuit design with its intake inside the building and its exhaust outside. The test section is 20 inches by 28 inches at the center and is 8 feet long. The prime mover is a six blade axial fan, located at the downstream end, driven by a variable speed, 75 horsepower motor. The wind speed is continuously variable from 30 to 300 feet-per-second.

IV. EXPERIMENTAL PROCEDURE

A. FLAT PLATE PREPARATION

To better monitor the surface temperature at various points on the flat plate, ten copper-constantin thermocouples were imbedded in the plate. The locations of the thermocouples are shown in Figures 1 and 3. The thermocouple bead was then covered with four coats of red glyptol to act as an electrical insulator. Prior to attachment of the flat plate, the temperature monitoring system consisting of the thermocouples, output meter, and connecting wires was calibrated using the Rosemount calibration bath.

A 12 by 9-7/16 inch area around the nozzle was covered with the electrically resistive Temsheet. The nominal thickness of the Temsheet was 0.038 inches, with an electrical resistance of approximately 45 ohms per square inch. The heat that is generated is uniform to within two percent from point to point over large areas when a constant electrical current is passed through a square section [31]. The Temsheet was marked in 1/8 inch increments laterally to provide a scale to determine the size of the disturbance area.

Originally, a spray adhesive was used to attach the Temsheet to the flat plate. However, during testing it was discovered that the adhesive melted at temperatures above 95°F, thus producing irregularities on the surface of the Temsheet

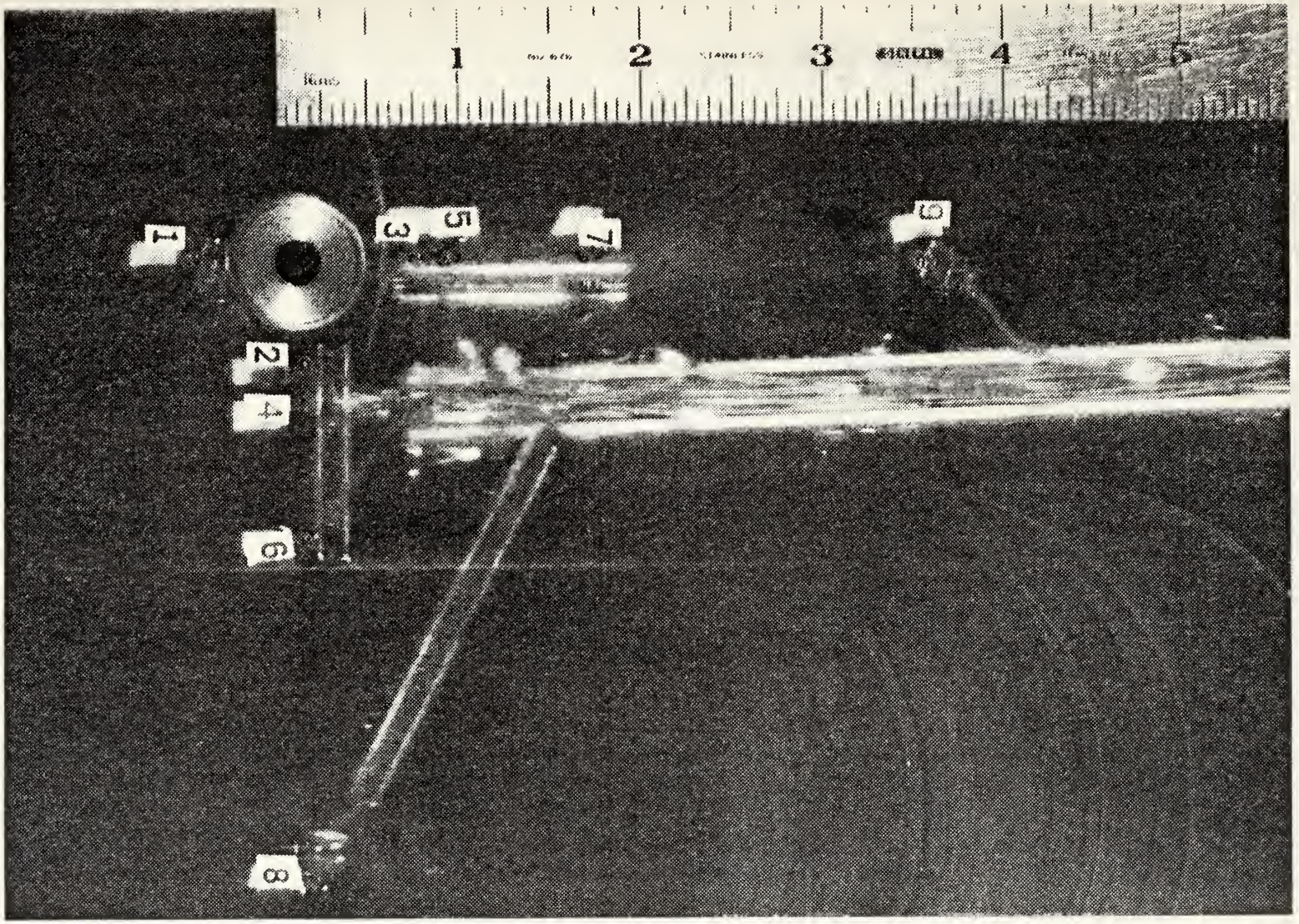

Figure 3. Location of Thermocouples 1-9 in Relation to Jet Nozzle.

which were displayed in the liquid crystal color transition. A double-sided adhesive tape proved to be a satisfactory substitute.

Self-adhering copper strips, attached to the edge of the Temsheet, served as connecting points for the power supply. Power to heat the Temsheet was provided by a Lambda model LK345A FM regulated D.C. power supply. The resistance of the system was measured and found to be 18.5 ohms.

The mixture of encapsulated cholesteric liquid crystals, which consisted of S-30, S-32, S-34, R-37, and distilled water, was sprayed onto the Temsheet using an air brush. Twelve coats of liquid crystals were necessary for satisfactory color production.

B. FLAT PLATE INSTALLATION

The flat plate was attached to 8-1/2 inch diameter disks constructed from plexiglas. The disks were fitted into the center of 20 by 29 inch plexiglas side panels, 1/2 inch thick. The flat plate and side panels were rigidly mounted in the low turbulence subsonic wind tunnel above a viewing window. The location of isotherms on the flat plate was photographically recorded with the aid of the distance markings placed on the Temsheet. Figure 4 shows the final setup in the plexiglas support frame.

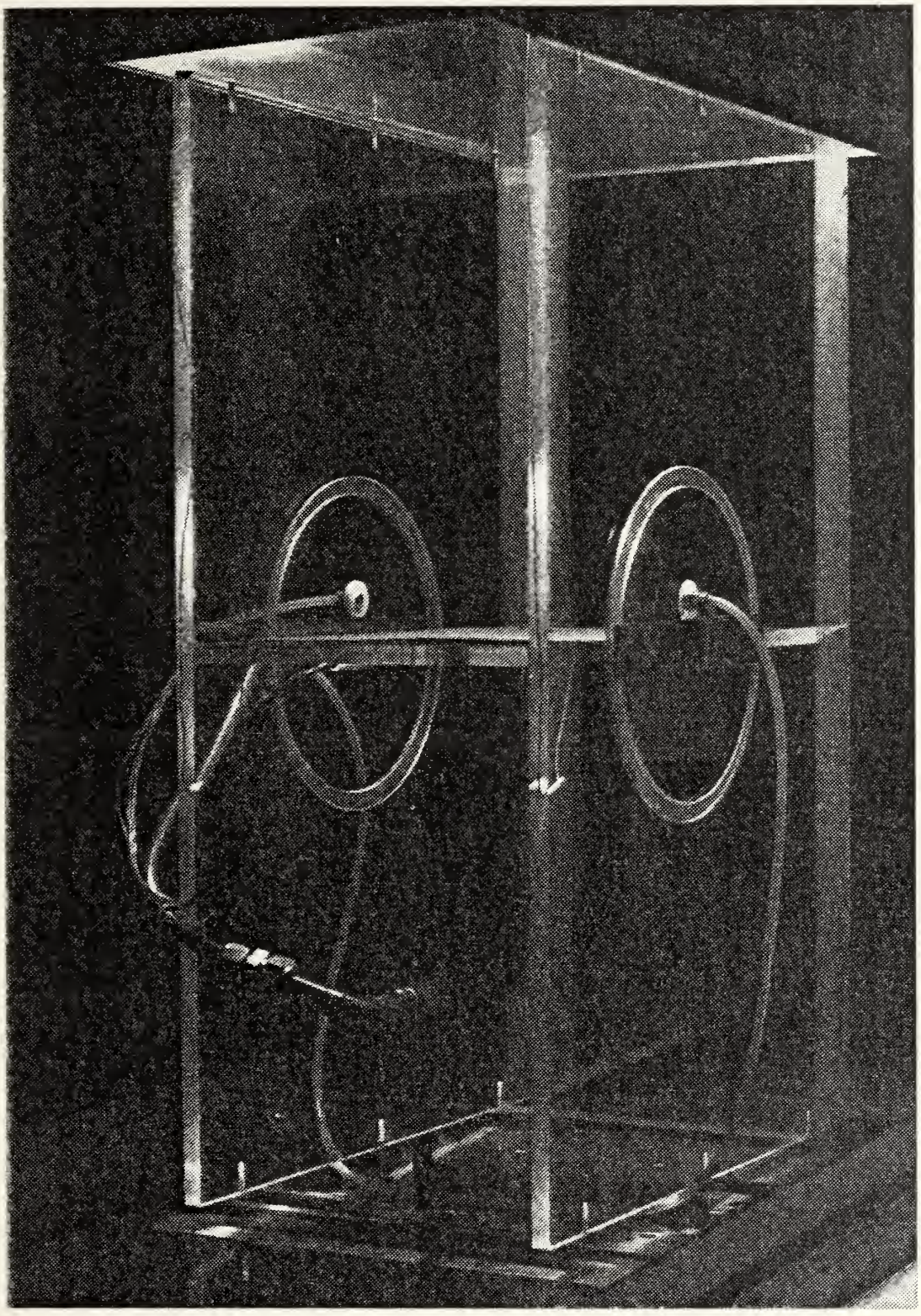

Figure 4. Final Test Arrangement Installed in Wind Tunnel.

C. FLAT PLATE SURFACE TEMPERATURE

The surface temperature on the flat plate was determined by the color of the liquid crystals. The thermocouples acted as an aid to determine which liquid crystal was actually being viewed. An increase or decrease in the applied voltage with jet and crossflow velocities held constant, raised or lowered, respectively, the average surface temperature of the flat plate. The thermocouples imbedded in the flat plate were monitored to insure steady state conditions when recording the surface temperatures.

D. PROCEDURE

Initially, the Temsheet was heated to various temperatures for a wide spectrum of jet-to-crossflow velocity ratios in order to attempt to picture the most enlightening liquid crystal display on the Temsheet. Since different heat inputs caused different plate temperature distributions, different liquid crystals would be active with each heating scheme. Additionally, for one heating scheme, different velocity ratios created different temperature distributions on the surface of the flat plate. Therefore, an optimum relationship between the two had to be reached. After considerable experimentation, it was determined that adjusting the voltage input to 49.0 volts (a heating power of 129.8 watts, Q/A equal to 99 watts/square foot) would ensure an adequate liquid crystal display over a wide range of velocity ratios.

A major portion of the testing was conducted at a wind tunnel (crossflow) velocity of 60 feet-per-second and at velocity ratios ranging from 1 to 7. Limited additional testing was conducted at crossflow velocities of 90 feet-per-second.

After heating the plate to an equilibrium temperature, photographs were taken of the natural cooling condition of the plate in the wind tunnel with no crossflow and no jet interaction. The jet alone was slowly added to observe its effects on the flat plate temperature distribution, and then, with no jet flow, the crossflow was initiated over the heated plate to observe its effects. With the crossflow at 60 feet-per-second, the jet was added again and its velocity was increased incrementally, allowing the plate to reach equilibrium between each incremental increase. Finally, the crossflow was increased to 90 feet-per-second and a similar investigation was conducted at three different velocity ratios.

V. RESULTS

Flow visualization studies of jets exhausting into crosswinds indicate that there is a high-pressure point near the front of the jet and that free-stream flow is deflected around the periphery of the jet into the wake region. In the region of the jet periphery, and particularly in the jet wake, some of the flow from the free stream gets sucked into the jet. These "blockage" and "entrainment" effects are the primary phenomenon that occur in the interaction between a jet and a crossflow. The jet produces a region of positive pressures upstream of the jet and a larger region of negative pressures laterally and downstream of the jet. The negative pressure field extends several jet diameters from the jet, is intensified by an increase in jet velocity, and is swept downstream by an increase in free-stream velocity [8]. The pressure distribution induced on the surface of a flat plate, as measured by Bradbury and Wood [13] for a velocity ratio of 4.0, is presented in Figure 5. The region of positive pressure ahead of the jet indicates a force augmenting the jet thrust. The large region of negative pressure adjacent to and aft of the jet indicates a force opposing the jet thrust to the side and behind the jet.

Figure 6 is a color photograph showing the liquid crystals previously discussed. The liquid crystals indicate the

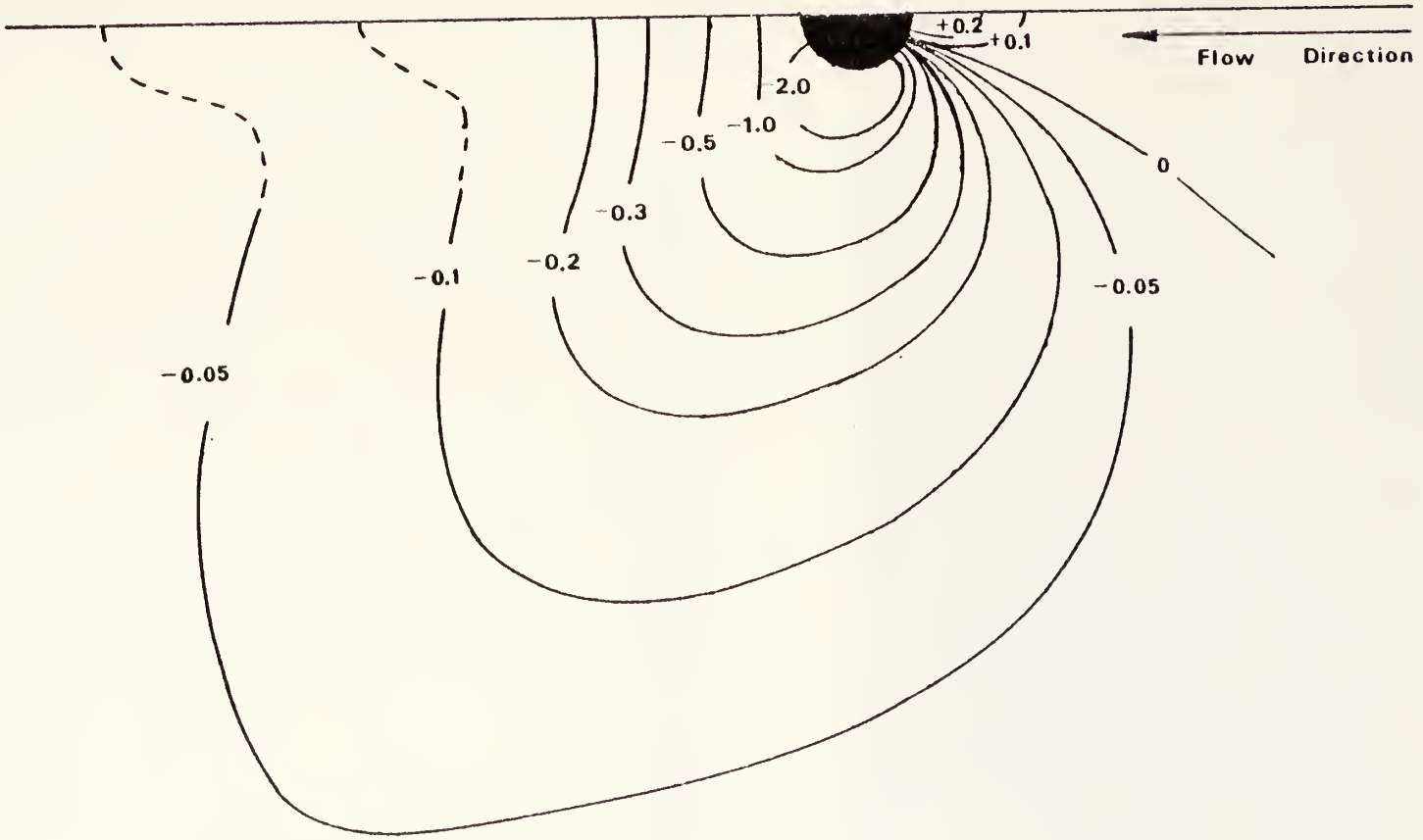

Figure 5. Pressure Distribution (Pressure Coefficients) on a Flat Plate at m = 4.0 [Ref. 13].

Figure 6. Temperature Distribution on Surface of Flat Plate at Zero Crossflow Velocity and Zero Jet Velocity.

natural cooling pattern around a hole (the jet opening) in a flat plate with no forced crossflow (there are natural convection currents) and no jet. Thermocouple readings are listed in Appendix A. Note the circular cooling pattern radiating from the hole and the heat loss along the edges of the Temsheet.

In viewing the isotherms generated by the liquid crystals in the following figures, it should be noted that because of the constant heat flux generated at the plate surface, the temperature difference between the surface and the free-stream flow is proportional to the convective film coefficient. This coefficient is dependent upon the velocity of the flow so that the temperature field indicated by the liquid crystals on the flat plate is reqresentative of the surface velocity field found there. Regions of high plate temperature will indicate relatively low velocities and vice versa. Therefore, with constant heat flux,

$$\frac{Q}{A} = h\Delta T = \text{constant}$$

which implies, $\Delta T \propto \frac{1}{h}$

$$h \propto Re^{n} \qquad n = 0.5 - 0.8$$

$$\Delta T \propto \frac{1}{U_{\infty}^{n}}$$

Utilizing Figure 6 as the natural or reference liquid crystal cooling pattern on the flat plate, the influence of a crossflow only and jet exhaust only was investigated.

Figure 7 shows the distortion made to the circular cooling pattern at a jet velocity of 200 feet-per-second with no crossflow. This distortion appears to be due to the secondary flow effects induced by jet entrainment in the presence of the side walls of the plexiglas support frame. As the jet air was exhausted into the test area, some of the fluid escaped longitudinally into the tunnel and had little cooling effect on the plate except very close to the jet opening. Other air was directed transversely against the side walls where it was recirculated, through entrainment, back up to the flat plate. The recirculation patterns were such that additional convective cooling resulted along a transverse portion of the plate in the region of the jet. If instead, the plate were of an infinite length and width and the flow was therefore unconfined, the cooling pattern would have remained symmetrical as in the zero jet velocity case of Figure 6.

Increasing the crossflow velocity with zero jet velocity leads to the development of a laminar boundary layer over the flat plate. Figure 8 shows the flat plate at a crossflow velocity of 60 feet-per-second. Assuming the critical Reynolds number for transition from laminar to turbulent flow on a flat plate is between $5x10^5$ and $5x10^6$, the critical length for a crossflow velocity of 60 feet-per-second is between 18 and 181 inches. As the boundary layer increases in thickness with distance from the leading edge of the Temsheet, the temperature

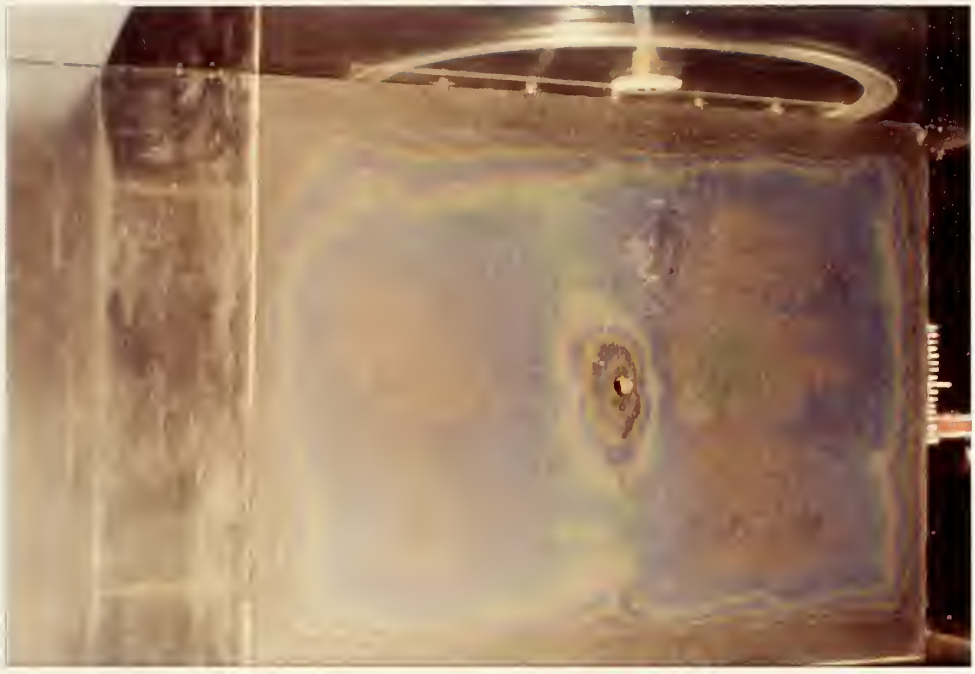

Figure 7. Temperature Distribution on Surface of Flat Plate with Jet Velocity 205 feet/second at Zero Crossflow Velocity.

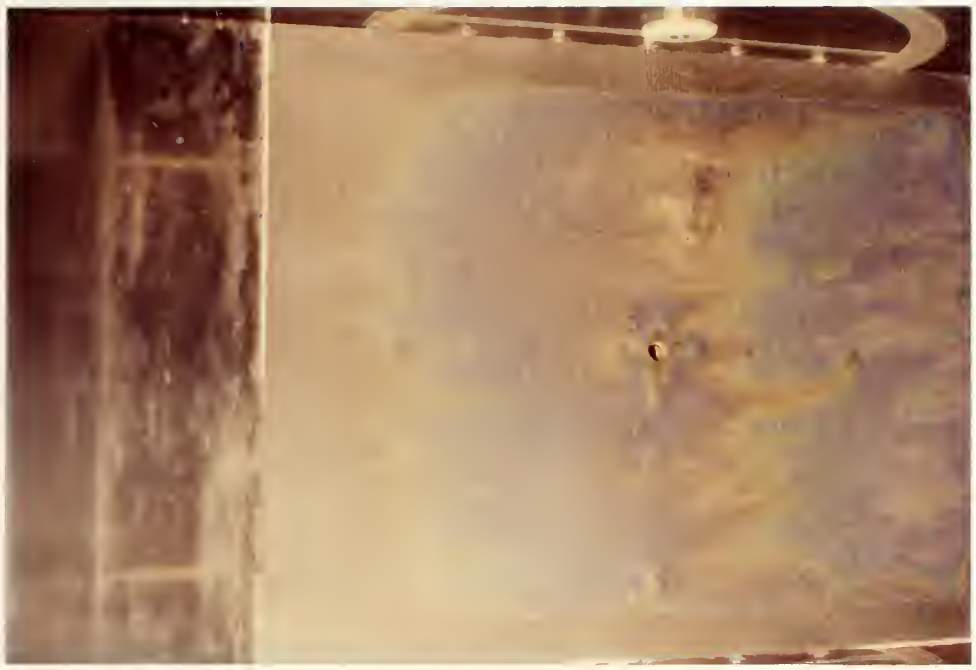

Figure 8. Temperature Distribution on Surface of Flat Plate with Crossflow Velocity 60 feet/second at Zero Jet Velocity.

of the plate increases. There is still a small cooling region noted around the jet opening. This cooling effect is attributed to flow impinging upon the jet opening and subsequently distorting the flow field around the opening.

While holding the heating power to the flat plate constant and maintaining the crossflow velocity at a constant 60 feet-per-second, the jet velocity was then varied over a wide range of velocity ratios. Figure 9 shows the velocity distribution on the flat plate at a velocity ratio, m = 1.0. The blockage effect described earlier can be seen in the near field region of the jet exhaust. More interesting to note is the far wake effect of the jet. Chislett and Bjorheden [19] have depicted the probable shape of the jet discharge and its accompanying pressure disturbance region, as indicated in Fig. 10, for different velocity ratios. The low velocity ratio is characterized by a deflected jet plume which lies close to or on the flat plate. The low velocity ratio illustrated in Fig. 10(c) produces a wake effect which can be seen in Figure 9 as cooling "spots" in the far wake region where the jet impinges on the plate.

As the jet velocity was increased, thus increasing the velocity ratio and causing the jet plume to detach from the flat plate, these cooling spots disappeared. The temperature profile of the region behind the jet also changed accordingly. The region of influence behind the jet gradually increased in size, resulting from the increased cooling induced by the

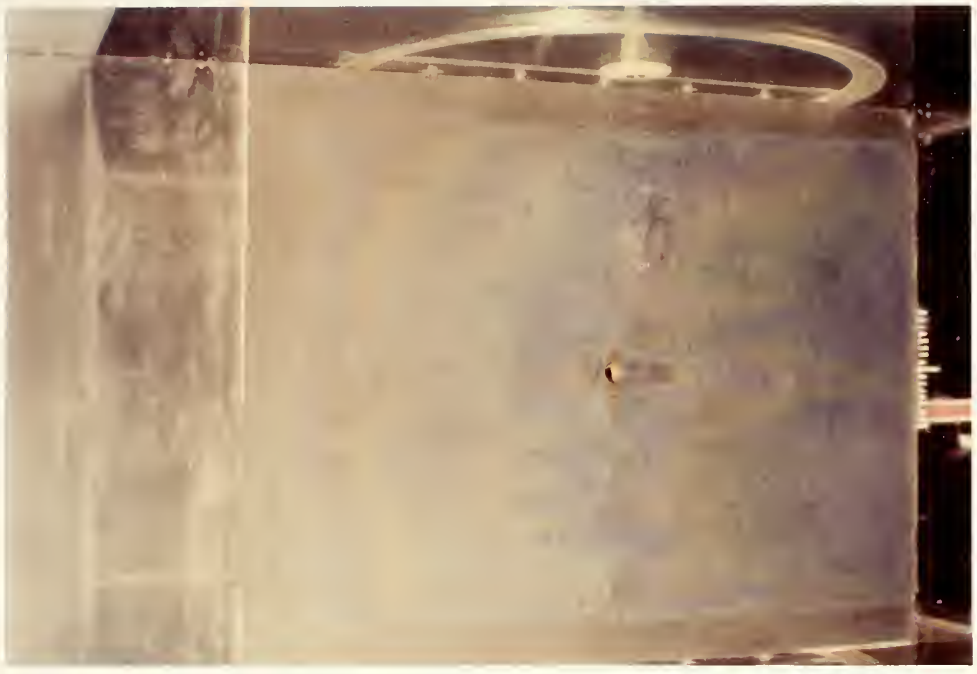

Figure 9. Temperature Distribution on Surface of Flat Plate at Crossflow Velocity 60 feet/second, m = 1.0.

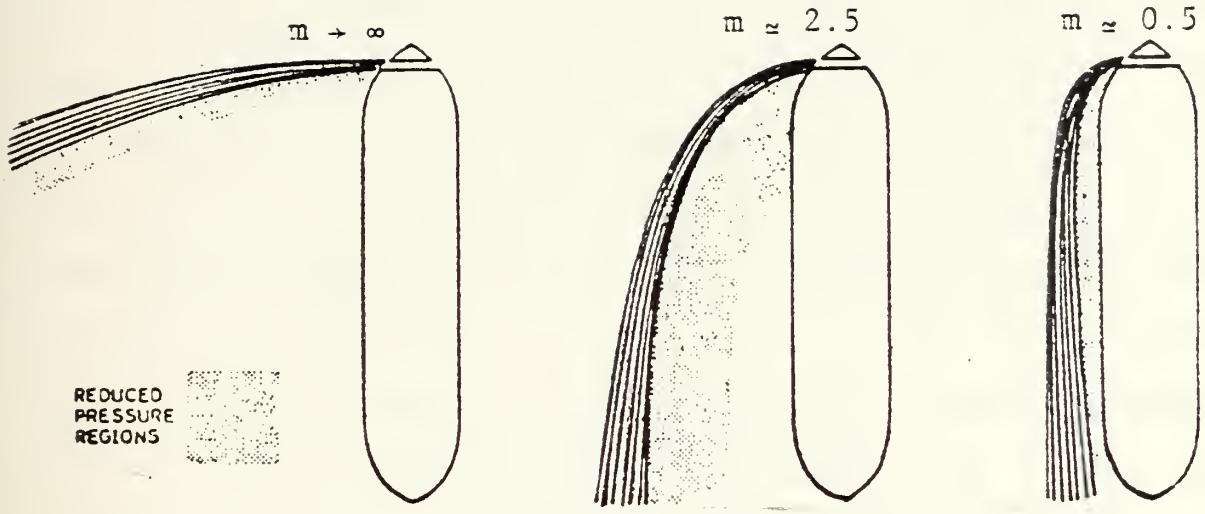

Figure 10. Probable Shape of Jet Discharge and Pressure Region [Ref. 19].

curved jet plume above the plate area behind the jet. Figure 11 shows the region of influence when the jet velocity was increased to 240 feet-per-second (m = 4.0).

Above a velocity ratio of about 4.25, an anomaly appeared to occur. Instead of an increased area of influence behind the jet and its accompanying cooling effect on the flat plate, the influence region began to shrink in size and the area behind the plate began to display a warming trend. This is shown in Figure 12. This phenomenon continued to a velocity ratio of 4.75. At higher velocity ratios the process reversed, once more increasing the size of the influence region behind the jet with increasing velocity ratios. Again, at a velocity ratio of approximately 5.25, the heating phenomenon returned and was again reversed at some point above m = 5.8. The reversing effect is considered an anomaly that should be investigated more closely. Additionally, an anomalous behavior in terms of pressure distributions has been observed by Fearn and Weston [17] at similar velocity ratios.

Limited testing was conducted at a crossflow velocity of 90 feet-per-second at velocity ratios of 1.0, 2.0, and 3.3. Although the minimum critical length for transition from laminar to turbulent flow decreased to 12 inches for a transition Reynolds number of 5×10^5 and it is possible that part of the flat plate was in the turbulent boundary layer, no visual evidence was indicated in the liquid crystal pattern. Similar far wake effects existed at m = 1.0 when compared to

Figure 11. Temperature Distribution on Surface of Flat Plate at Crossflow Velocity 60 feet/second, m = 4.0.

Figure 12. Temperature Distribution on Surface of Flat Plate at Crossflow Velocity 60 feet/second, m = 4.75.

the previous flow at 60 feet per second and disappeared as the velocity ratio increased. Figure 13 shows the effect of the jet plume in the far wake region. As the velocity ratio was increased, similar temperature profiles were obtained on the surface of the flat plate to those obtained at a cross-flow velocity of 60 feet-per-second with the same velocity ratio.

As a significant point of interest, strong visual similarities existed between the temperature distribution on the flat plate, as depicted by the liquid crystals, and the theoretical surface velocity field around a jet modelled as a symmetrical foil near the point of injection and a vortex sheet in the plumes. For a velocity ratio of 4.0, this theory[1] predicts the surface velocity distribution shown in Figure 14. As would be expected, regions of high velocity (to the sides and aft of the jet in Figure 14) exhibited cooling trends in the thermal maps. In the low velocity regions (forward of the jet in Figure 14) relatively high temperatures were indicated. Most remarkable, perhaps, was the verification (Figures 9, 11-13) by means of liquid crystal thermography of the general shape and extent of the interaction region predicted by the theory.

---

[1]The theoretical development is a complementary phase of the general investigation of bow thrusters and will appear in the thesis of LCDR T. C. Cooper to be published.

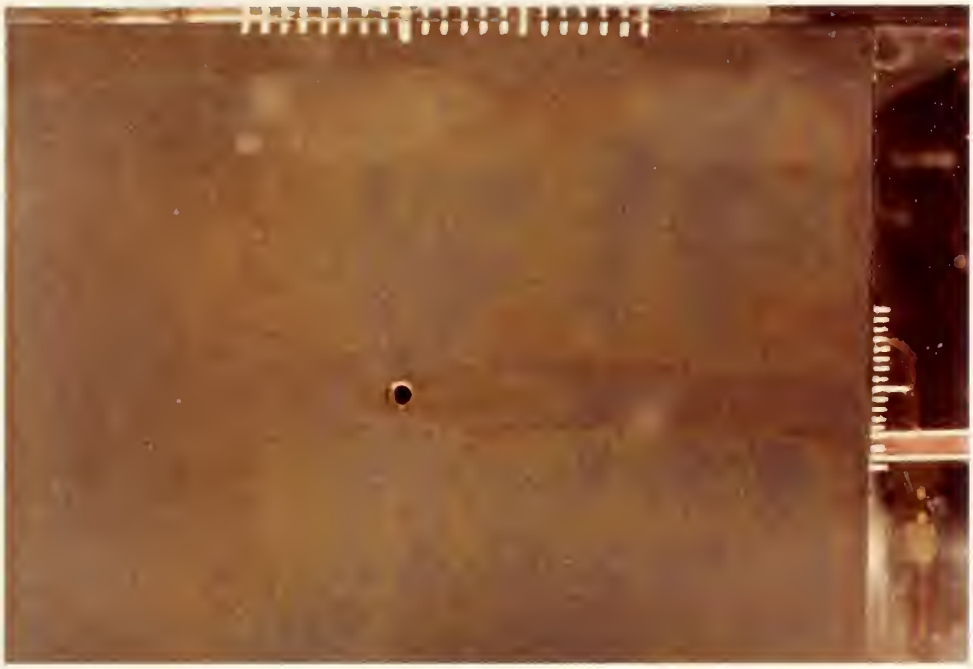

Figure 13. Temperature Distribution on Surface of Flat Plate at Crossflow Velocity 90 feet/second, m = 1.0.

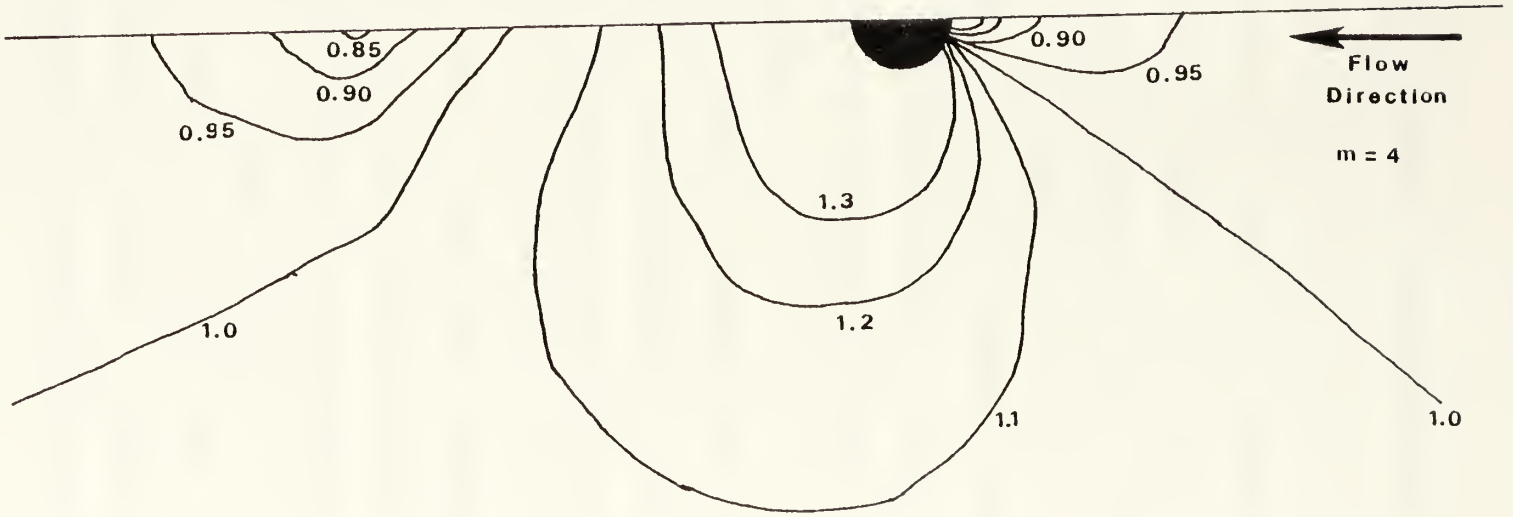

Figure 14. Theoretical Surface Velocity Field Around a Jet Modelled as a Symmetrical Foil near the Point of Injection and a Vortex Sheet in the Plumes.

VI. CONCLUSIONS AND RECOMMENDATIONS

The liquid crystal thermographic technique developed in this investigation indicates that a qualitative description of the disturbance field created on the surface of a flat plate from which a jet was injected into a crossing flow can be determined. It was possible to visualize the various temperature distributions on the surface of the flat plate for different jet-to-crossflow velocity ratios utilizing the technique. Liquid crystals allowed continual visual observation of the cooling effects of the jet as jet velocity was slowly increased with crossflow velocity and power to the Temsheet held constant. Additionally, the technique showed the cooling pattern similarities that exist at the same velocity ratios for different crossflow velocities.

The ability to visually observe the temperature distribution on the surface of the flat plate suggests an excellent means for studying the entire near field disturbance zone of a jet exhausting into a crossing stream. Visual similarities exist between the theoretical velocity field and the temperature distribution on the flat plate. A relationship may also exist between the temperature distribution and the pressure distribution.

To allow a quantitative study (utilizing the pressure distribution on the flat plate), pressure taps are needed in

order to correlate pressures to temperatures. Additional thermocouples should also be mounted to better identify which liquid crystals are active and to more easily determine the temperature distribution on the flat plate.

There is much speculation as to the exact nature of the interaction between the jet and crossflow at different velocity ratios. The sole use of liquid crystals is inadequate to completely describe the reasons behind the influence field around the jet. While the temperature distribution on the flat plate is well depicted, any explanation for a particular cooling pattern is left to the intuition and deduction of the observer. For this reason, flow visualization is needed to properly identify the jet path and any disturbances created by the jet exhausting into the crossflow.

Future studies need to be conducted expanding the present investigation. Crossflow velocities should be increased, utilizing the same jet-to-crossflow velocity ratios, in order to determine if temperature patterns on the surface of the flat plate change or if they are solely dependent on velocity ratios, as surmised by other investigators. Tests could also be conducted at higher velocity ratios to see if the pattern is consistent at higher jet velocities. Additionally, a more thorough investigation should be conducted over velocity ratio ranges of 4.0 to 6.0 to attempt to properly identify the ratios where the anomalous behavior, described earlier, occurs.

As this technique becomes more refined, investigations may be conducted to attempt to determine the most effective bow thruster design. Since duct diameter is a major factor in the installation cost and operating efficiency of the bow thruster [28], jet diameters should be varied for the same velocity ratios and comparisons made. Similarly, the shape of the duct opening may be varied to see what influence a sharp-edged outlet has on the plate temperature as compared to a faired lip outlet [26, 28]. It is normal in the ship-building industry to place two small thrusters side by side when the use of a larger diameter thruster is not feasible because of draft limitations or the thruster size is prohibitive [2, 27]. An investigation may be conducted to determine the effects this has on the interference field of the flat plate. Angling the thruster outflow to exhaust more directly into the crossflow could also improve thruster performance [7] and this geometry could be investigated.

Experiment indicates that extending the thruster duct beyond the hull (as in the form of a retractable tube extension) reduces the suction effect on the hull created by the jet-crossflow interaction [25]. Such an extension would be an interesting investigation using the liquid crystal thermography technique.

A more direct application of the current technique as related to bow thrusters could be to apply the Temsheet and liquid crystals to a model ship's hull form installed in the

wind tunnel and conduct investigations similar to those described here. The location of the duct opening could also be shifted along the hull, moving it more forward, more aft, closer to the keel, and closer to the waterline to see if duct location h as a major influence on the temperature field created by the jet-crossflow interaction [28].

The difficulty and inconvenience involved in attaching a Temsheet to a test surface and formulating and spraying liquid crystals onto the Temsheet make it impractical to use as a routine investigative tool in the design and testing of bow thrusters. Hippensteele, et al. [36] have developed a layered composite consisting of a plastic sheet coated with liquid crystals and a heater sheet which they found to provide a more simple, more convenient, equally accurate, and reasonably low-cost description of the temperature changes. As a final consideration, their evaluation should be closely examined as a possible follow-up technique utilizing the methods described in the present study.

APPENDIX A

SUPPORTING DATA

CROSSFLOW VELOCITY 0 feet/second

JET-TO-CROSSFLOW VELOCITY RATIO 0/0

HEATING POWER TO FLAT PLATE 48.6 watts

THERMOCOUPLE READINGS (°F) (Fig. 6)

1)	86.1
2)	84.8
3)	88.8
4)	88.9
5)	91.3
6)	92.4
7)	95.3
8)	90.0
9)	95.6
10)	92.8

CROSSFLOW VELOCITY 0 feet/second

JET-TO-CROSSFLOW VELOCITY RATIO $\rightarrow \infty$ (jet velocity 205 ft/sec)

HEATING POWER TO FLAT PLATE 28.1 watts

THERMOCOUPLE READINGS (°F) (Fig. 7)

1)	82.4
2)	81.9
3)	88.4
4)	86.4
5)	90.8
6)	90.7
7)	94.6
8)	90.3
9)	93.2
10)	92.9

CROSSFLOW VELOCITY 60 feet/second

JET-TO-CROSSFLOW VELOCITY RATIO 0

HEATING POWER TO FLAT PLATE 86.5 watts

THERMOCOUPLE READINGS (°F) (Fig. 8)

1)	82.9
2)	79.2
3)	82.5
4)	81.8
5)	83.5
6)	81.9
7)	83.6
8)	82.7
9)	85.6
10)	80.4

CROSSFLOW VELOCITY 60 feet/second

JET-TO-CROSSFLOW VELOCITY RATIO 1.0

HEATING POWER TO FLAT PLATE 129.8 watts

THERMOCOUPLE READINGS (°F) (Fig. 9)

1)	86.5
2)	80.6
3)	81.7
4)	83.8
5)	82.9
6)	84.5
7)	84.6
8)	86.4
9)	88.8
10)	82.9

CROSSFLOW VELOCITY 60 feet/second

JET-TO-CROSSFLOW VELOCITY RATIO 4.0

HEATING POWER TO FLAT PLATE 129.8 watts

THERMOCOUPLE READINGS (°F) (Fig. 11)

1) 85.4

2) 79.6

3) 79.1

4) 83.5

5) 80.7

6) 84.6

7) 82.8

8) 85.7

9) 86.8

10) 83.1

CROSSFLOW VELOCITY 60 feet/second

JET-TO-CROSSFLOW VELOCITY RATIO 4.75

HEATING POWER TO FLAT PLATE 129.8 watts

THERMOCOUPLE READINGS (°F) (Fig. 12)

1) 85.3

2) 79.6

3) 79.1

4) 83.5

5) 80.7

6) 84.8

7) 83.1

8) 85.9

9) 87.5

10) 83.0

CROSSFLOW VELOCITY 90 feet/second

JET-TO-CROSSFLOW VELOCITY RATIO 1.0

HEATING POWER TO FLAT PLATE 109.5 watts

THERMOCOUPLE READINGS (°F) (Fig. 13)

1) 77.1

2) 87.9

3) 75.8

4) 87.8

5) 77.2

6) 85.8

7) 80.5

8) 86.2

9) 83.4

10) not available

LIST OF REFERENCES

1. Foulerton, Robert, "A Letter to the Lords of the Admiralty on the Ship Maneuver," Thomas Dean and Co., London, 1846.

2. Norrby, Ralph A. and Ridley, Donald E., "Notes on Thrusters for Ship Maneuvering and Dynamic Positioning," Trans. SNAME, Vol. 88, 1980.

3. English, J.W., "The Design and Performance of Lateral Thrust Units for Ships, Hydrodynamic Considerations," Trans. RINA, Vol. 105, 1963.

4. Jordinson, R., "Flow in a Jet Directed Normal to the Wind," R&M No. 3074, British A.R.C., 1958.

5. Gordier, R.L., "Studies on Fluid Jets Discharging Normally into Moving Liquid," St. Anthony Falls Hyd. Lab., Tech. Paper No. 28, Series B, August 1959.

6. Keffer, J.F., and Baines, W.D., "The Round Turbulent Jet in a Cross-Wind," Journal of Fluid Mechanics, Vol. 15, April 1963.

7. Margason, Richard J., "The Path of a Jet Directed at Large Angles to a Subsonic Free Stream," NASA TN D-4919, 1968.

8. Keffer, James F., "The Physical Nature of the Subsonic Jet in a Cross-Stream," NASA SP-218, 1969.

9. Wooler, P.T., "Flow of a Circular Jet into a Cross Flow," Journal of Aircraft, Vol. 6, No. 3, 1969.

10. Stoy, R.L., and Ben-Haim, Y., "Turbulent Jets in a Confined Crossflow," Journal of Fluids Engineering, December 1973.

11. Sucec, J., and Bowley, W.W., "Prediction of the Trajectory of a Turbulent Jet Injected into a Crossflowing Stream," Journal of Fluids Engineering, December 1976.

12. Vogler, Raymond D., "Surface Pressure Distributions Induced on a Flat Plate by a Cold Air Jet Issuing Perpendicularly from the Plate and Normal to a Low-Speed Free-Stream Flow," NASA TN D-1629, 1963.

13. Bradbury, L.J.S., and Wood, M.N., "The Static Pressure Distribution around a Circular Jet Exhausting Normally from a Plane Wall into an Airstream," C.P. No. 822, British A.R.C., 1965.

14. Wooler, P.T., Burghard, G.H., and Gallagher, J.T., "Pressure Distribution on a Rectangular Wing with a Jet Exhausting Normally into an Airstream," Journal of Aircraft, Vol. 4, 1967.

15. McMahon, Howard M., and Mosher, David K., "Experimental Investigation of Pressures Induced on a Flat Plate by a Jet Issuing into a Subsonic Crosswind," NASA SP-218, 1969.

16. Kamotani, Y., and Greber, I., "Experiments on a Turbulent Jet in a Crossflow," AIAA Journal, Vol. 10, No. 11, November 1972.

17. Fearn, Richard L., and Weston, Robert P., "Induced Pressure Distribution of a Jet in a Crossflow," NASA TN D-7916, 1975.

18. Bergeles, G., Gosman, A.D., and Launder, B.E., "The Near-Field Character of a Jet Discharged Normal to a Main Stream," Journal of Heat Transfer, August 1976.

19. Chislett, M.S., and Bjorheden, O., "Influence of Ship Speed on the Effectiveness of a Lateral-Thrust Unit," Hydro-Og Aerodynamisk Laboratum, Lyngby, Denmark, Report No. HY-8, April 1966.

20. Wooler, P.T., "On the Flow Past a Circular Jet Exhausting at Right Angles from a Flat Plate or Wing," Journal of the Royal Aeronautical Society, Vol. 71, March 1967.

21. Wu, J.C., and Wright, M.A., "A Blockage-Sink Representation of Jet Interference Effects for Noncircular Jet Orifices," NASA SP-218, 1969.

22. Waterman, Bradford Bates, III, "Analysis of Jet-Crossflow Interactions with Application to Ship Bow Thrusters," MSME Thesis, Naval Postgraduate School, Monterey, California, 1980.

23. Stuntz, George R., and Taylor, Robert J., "Some Aspects of Bow-Thruster Design," Trans. SNAME, Vol. 72, 1964.

24. Norrby, Ralph, "The Effectiveness of a Bow Thruster at Low and Medium Ship Speeds," International Shipbuilding Progress, Vol. 14, No. 156, August 1967.

25. Beveridge, John L., "Bow Thruster Jet Flow," Journal of Ship Research, Vol. 15, No. 3, September 1971.

26. English, J.W., "Further Considerations in the Design of Lateral Thrust Units," International Shipbuilding Progress, Vol. 13, No. 137, January 1966.

27. Dewhurst, Peter K., "Experience in the Control of Ships by Right Angle Drive Thrusters," Naval Engineers Journal, August 1970.

28. Beveridge, John L., "Design and Performance of Bow Thrusters," NSRDC Report 3611, September 1971.

29. Fergason, James L., "Liquid Crystals," Scientific American, Vol. 211, No. 2, August 1964.

30. Klein, E.J., "Liquid Crystals in Aerodynamic Testing," Astronautics and Aeronautics, Vol. 6, No. 7, July 1968.

31. Cooper, T.E., Field R.J., and Meyer, J.F., "Liquid Crystal Thermography and its Application to the Study of Convective Heat Transfer," Journal of Heat Transfer, Vol. 97, No. 3, August 1975.

32. McElderry, E.D., "Boundary Layer Transition at Supersonic Speeds Measured by Liquid Crystals," Air Force Flight Dynamics Laboratory, FDMG Tm 70-3, June 1970.

33. Brennon, Roy L., "Investigation of the Use of Liquid Crystal Thermography to Study Flow over Turbomachinery Blades," MSME Thesis, Naval Postgraduate School, Monterey, California, 1980.

34. Field, R.J., "Liquid Crystal Mapping of the Surface Temperature on a Heated Cylinder Placed in a Crossflow of Air," MSME Thesis, Naval Postgraduate School, Monterey, California, 1974.

35. Durao, M.C., "Investigation of Heat Transfer in Straight and Curved Rectangular Ducts Using Liquid Crystal Thermography," ENGR Thesis, Naval Postgraduate School, Monterey, California, 1977.

36. Hippensteele, Steven A., Russell, Louis M., and Stepka, Francis S., "Evaluation of a Method for Heat Transfer Measurements and Thermal Visualization Using a Composite of a Heated Element and Liquid Crystals," NASA TM-81639, 1981.

INITIAL DISTRIBUTION LIST

		No. Copies
1.	Defense Technical Information Center Cameron Station Alexandria, Virginia 22314	2
2.	Library, Code 0142 Naval Postgraduate School Monterey, California 93940	2
3.	Department Chairman, Code 69 Department of Mechanical Engineering Naval Postgraduate School Monterey, California 93940	1
4.	Professor R. H. Nunn, Code 69Nn Department of Mechanical Engineering Naval Postgraduate School Monterey, California 93940	1
5.	LT Michael David Johnson, USN P.O. Box 531 Wendell, North Carolina 27591	1

197728
Thesis
J6239 Johnson
c.1 Liquid crystal mapping of jet crossflow interactions.